ARTICLES

Carbon−Oxygen Bond Strength in Diphenyl Ether and Phenyl Vinyl Ether: An Experimental and Computational Study

Wibo van Scheppingen, Edwin Dorrestijn, Isabel Arends, and Peter Mulder*

Center for Chemistry and the Environment, Leiden Institute of Chemistry, Leiden University, P.O. Box 9502, 2300 RA Leiden, The Netherlands

Hans-Gert Korth*

Universität Essen, Institut für Organische Chemie, Universitätsstrasse 5, D-45117 Essen, Germany

Received: February 4, 1997; In Final Form: April 8, 1997[⊗]

The thermal decomposition of gaseous diphenyl ether (DPE) and phenyl vinyl ether (PVE) has been studied, at atmospheric pressure in hydrogen and in a very low-pressure reactor, over a temperature range of 1050−1200 K. The high-pressure rate constant for homolytic bond cleavage $C_6H_5O-C_6H_5 \rightarrow C_6H_5O^{\bullet} + C_6H_5^{\bullet}$ (1) obeys k_1 (s^{-1}) = $10^{15.50}$ exp(−75.7/*RT*). Two pathways can be distinguished for $C_6H_5OC_2H_3$: $C_6H_5^{\bullet} + C_2H_3O^{\bullet}$ (2) and $C_6H_5O^{\bullet} + C_2H_3^{\bullet}$ (3). The overall rate constant follows k_{2+3} (s^{-1}) = $10^{15.50}$ exp(−73.3/*RT*). The rate ratio, v_2/v_3, amounts to 1.8 and appears to be temperature independent. These findings result in bond dissociation energies (BDE) at 298 K for $C_6H_5O-C_6H_5$, $C_6H_5-OC_2H_3$, and $C_6H_5O-C_2H_3$ of 78.8, 75.9, and 76.0 kcal mol^{-1}, respectively. The enthalpies for reactions 1−3 have been also determined at 298 and 1130 K by *ab-initio* calculations using the density functional theory formalism on the B3LYP/6-31G(d) and B3LYP/6-311++G(d,p) level. Comparison between experiments and theoretical calculations reveals distinct variances (ca. 3−4 kcal mol^{-1}) for the BDE(C−O) in aryl ethers and the BDE(O−H) in phenol and vinyl alcohol but a close agreement for the BDE(C−H) in the related hydrocarbons: toluene, benzene, and ethene.

Introduction

Accurate knowledge of the strength of a particular bond in a chemical compound is of vital importance to understand the chemical reactivity in photochemically or thermally initiated homolytic bond cleavage processes. Also, bond dissociation energy (BDE) considerations can be used to explain differences in, for example, bimolecular hydrogen abstraction rates in a series of related compounds.[1] A number of methods for the determination of BDEs are available, each with its intrinsic limitations: gas phase studies using rates of bond cleavage at elevated temperature or appearance potential measurements and studies in the liquid phase by electrochemical or photoacoustic methods.[2] A recent survey[3] presents high-quality BDE values for mostly carbon−carbon and hydrogen−carbon bonds in aliphatic, vinylic and aromatic compounds.

However, due to all kinds of experimental constraints, direct determination of a specific bond strength in complex polysubstituted compounds is often not conceivable. In such cases, classical group additivity rules have proven to be instrumental in enthalpy assessments. Moreover, high level *ab-initio* computational studies are becoming increasingly practical and reliable. In this context advanced density functional theory (DFT) calculations provide a very promising tool.

In the recent years we have studied the thermal behavior of acyclic and cyclic aryl ethers as model compounds to determine absolute BDE values for the different carbon−phenoxyl linkages.[4] In general, the thermal reactivity of aryl ethers is of interest to various fields of chemistry since these structures are present as base units in natural polymeric materials like lignin and coal. They have been identified as key precursors for the formation of dibenzodioxins and dibenzofurans during thermal (combustion) processes.[5] The strength of the alkyl−phenoxyl bond is, relative to other carbon−oxygen bonds, substantially lowered due to the resonance stabilization in the product (phenoxyl) radical. Stronger carbon−oxygen bonds can be expected with two sp^2 carbons adjacent to oxygen such as in diphenyl ether (DPE) and phenyl vinyl ether (PVE).

The thermal decomposition of diphenyl ether has been studied before[6] in coal-related systems, and BDEs ranging from 76 to 80 kcal mol^{-1} have been reported. Homolytic bond cleavage of the aryl−oxygen bond in DPE only yields the phenyl and the phenoxyl radical (1).

$$C_6H_5O-C_6H_5 \rightarrow C_6H_5O^{\bullet} + C_6H_5^{\bullet} \quad (1)$$

In the case of PVE two competitive routes can be identified: rupture of the phenyl−oxygen (2) or the vinyl−oxygen bond (3):

$$C_6H_5-OC_2H_3 \rightarrow C_6H_5^{\bullet} + {}^{\bullet}OCHCH_2 \quad (2)$$

$$C_6H_5O-C_2H_3 \rightarrow C_6H_5O^{\bullet} + {}^{\bullet}CHCH_2 \quad (3)$$

With the recommended heats of formation of the product radicals,[3] an enthalpy consideration predicts that the $\Delta_r H_{298}$ for reaction 3 is around 2 kcal mol^{-1} higher than for reaction 2. This calculation implies that the C−H bonds in ethene and benzene are equally strong. However, in view of the uncertain-

* Corresponding author. E-mail: P.Mulder@Chem.LeidenUniv.NL.
⊗ Abstract published in *Advance ACS Abstracts,* June 15, 1997.

S1089-5639(97)00432-5 CCC: $14.00

ties associated with enthalpy assessments, a (experimental) study on the branching ratio is the most straightforward approach to confirm or to refine these thermochemical quantities.

In this investigation two methods have been applied. Both compounds, DPE and PVE, have been subjected to a thermolytic study between 1050 and 1200 K with hydrogen as the bath gas, at short residence times with the emphasis on unimolecular rate constants and products. Experiments were also performed under very low-pressure pyrolysis (VLPP) conditions to ensure a unimolecular behavior. Subsequently, calculations have been performed, using density functional theory at the B3LYP/6-31G(d) and B3LYP/6-311++G(d,p) levels, to derive vibrational frequencies and thermodynamic quantities for (1), (2), and (3) at 298 and 1130 K. In this way a data set is created that allows a direct evaluation and comparison of experimental and theoretical determined thermochemical values for relatively large species.

Experimental Section

Thermolysis Experiments at Atmospheric Pressures. Thermal decomposition of DPE was performed in a flow apparatus as described previously,[4a] using a 31 μL quartz tubular reactor and short residence times ($\tau \cong 24$ ms) over a temperature range of 1123−1168 K. Typically, the entrance gas mixture consisted of aryl ether (0.24%), nitrogen (13.96%), and hydrogen (85.80%). CH_4 was added as calibration gas to the exit stream; reactant and products profiles were quantified by on-line GC measurements. Blank runs were recorded at 523 K.

The experiments with PVE were performed, using a capillary reactor of 21 μL, between 1020 and 1160 K with residence times of ca. 10 ms. Nitrogen gas was used as carrier gas (70−93%) together with hydrogen and/or chloromethane as hydrogen donors. The intake of PVE ranged from 0.04 to 0.08%. No separate calibration gas was added because methane appeared to be a reaction product.

Very Low-Pressure Pyrolysis. Reactions were performed with a newly developed instrument similar to those described before.[7] The reagent was introduced in a Knudsen quartz reaction chamber of 28.1 mL via a glass capillary by means of sublimation (DPE at 21 °C) or vaporization (PVE at 0 °C). The pressure inside the reaction vessel was regulated by adjusting the flow rate of the reagent with a regulating valve (Nupro) and measured with a Baratron pressure transducer (MKS). The reactor was heated by a tube furnace (Carbolite) with an internal diameter of 25 mm. The temperature was measured with a chromel−alumel thermocouple placed inside the reactor via a quartz insert. The vacuum of the system was maintained by an oil diffusion pump (Edwards).

After escape through a single aperture (diameter 1.2 mm) the molecular beam was sampled continuously by a HP 5970 mass selective detector (Hewlett-Packard). The spectra over $m/z = 10-200$ (PVE) and 10−175 (DPE) were recorded using an ionization energy of 18 eV to reduce fragmentation of the reagent and products. After temperature equilibration, 200−440 scans were averaged to improve the signal/noise ratio. Intensities were corrected for amounts that arose from the fragmentation of the starting compound as recorded during a blank run at 873 K. In case of PVE, experiments were repeated over a range of pressures (0.5−5 mTorr) to verify unimolecular behavior.

Chemicals. Diphenyl ether (Merck, >99%) was used as received. Phenyl vinyl ether was synthesized[8] from β-bromophenetole (Aldrich, >99%). Treatment with potassium-*tert*-butoxide in dimethyl sulfoxide as the solvent at room temperature for 2 h gave phenyl vinyl ether with 98% purity (GC).

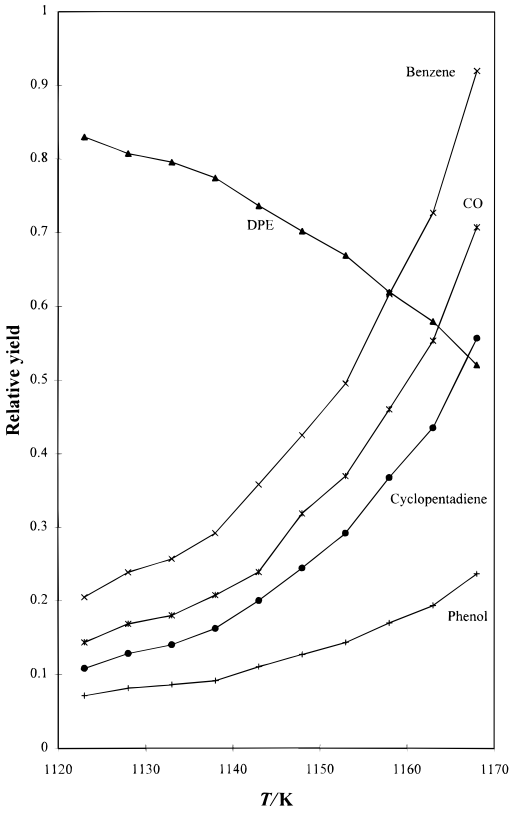

Figure 1. Product distribution for unimolecular decomposition of diphenyl ether (DPE) in hydrogen at atmospheric pressures.

Chloromethane (99.5%) and methane (99.995%) were used as such. Hydrogen and nitrogen were passed through moisture and charcoal filters prior to use.

Computational Procedures. Density functional theory[9] calculations were performed with the Gaussian 94 suite of programs[10] on a IBM RS6000 computer and a Silicon Graphics Indy workstation. Structures were fully optimized to stationary points by restricted (for closed-shell molecules) or unrestricted (for radicals) calculations employing the B3LYP functionals[11] on the 6-31G(d) and 6-311++G(d,p) basis sets. In the calculations on the radicals the value for the spin operator $\langle S^2 \rangle$ never exceeded 0.789 (phenoxyl) and was reduced to below 0.751 after annihilation of the first (quartet) spin contaminant. Zero-point vibrational energies and thermochemical data were evaluated by frequency calculations on the same levels of theory for temperatures of 298 K and, in part, 1130 K. Anharmonicity of the molecular vibrations was taken into account by using a correction factor of 0.97 for the calculated vibrational frequencies.[12] On the B3LYP/6-31G(d) level, computation of DPE afforded about 56 h CPU time for five optimization cycles and the frequency job. Therefore, only compounds up to the size of phenol were calculated with the larger 6-311++G(d,p) basis set, consuming, *e.g.*, about 32 h CPU time for phenoxyl.

Results

DPE and PVE Thermolysis in Hydrogen. The product pattern during the DPE thermolysis[13] consisted of benzene, phenol, carbon monoxide, and cyclopentadiene as the main products according to reactions 1 and 4−7 (see Figure 1).

$$C_6H_5^{\bullet} + H_2 \rightarrow C_6H_6 + H^{\bullet} \quad (4)$$

$$C_6H_5O^{\bullet} + H_2 \rightarrow C_6H_5OH + H^{\bullet} \quad (5)$$

$$C_6H_5O^{\bullet} \rightarrow C_5H_5^{\bullet} + CO \quad (6)$$

$$C_5H_5^{\bullet} + H_2 \rightarrow C_5H_6 + H^{\bullet} \quad (7)$$

Minor products included dibenzofuran (DF) and *o*-hydroxybiphenyl (OHB), as well as (methyl) indene and (methyl) naphthalene. The latter compounds (ca. 1% with respect to benzene) have also been observed in phenol hydrogenolysis and can be associated with cyclopentadienyl chemistry.[14]

The overall rate constant ($k_{ov,DPE}$) for the conversion of diphenyl ether was calculated from the benzene formation by forcing the phenyl balance to unity; hence, $[DPE]_{out} + [C_6H_6]_{out} = [DPE]_{in}$ and $k_{ov,DPE} = -(1/\tau)\ \ln\{[DPE]_{out}/([DPE]_{out} + [C_6H_6]_{out})\}$. Experimentally, the absolute phenyl mass balance was found to be slightly lower, ranging from 98.7 to 97.4%. Accordingly, the derived kinetic expression followed $k_{ov,DPE}/s^{-1} = 10^{15.4} \exp(-74.9/RT)$. The *A* factor points strongly to a homolytic decomposition.

Since hydrogen atoms were present in the reaction mixture, a possible contribution of an additional bimolecular decomposition route for DPE by hydrogen atoms might perturb the unimolecular decay. *Ipso* addition yields reaction products that are identical to those for the homolytic cleavage, i.e., benzene and phenoxyl (reaction 8):

$$C_6H_5OC_6H_5 + {}^{\bullet}H \rightarrow C_6H_6 + C_6H_5O^{\bullet} \quad (8)$$

To assess the contribution of (8), the following assumption was made: the hydrogen atom concentration is determined by the equilibrium constant[15] for dissociation of molecular hydrogen into two hydrogen atoms. In this temperature region and with the applied $[H_2]$, the $[H^{\bullet}]$ increased from $10^{-9.53}$ M at 1123 K to $10^{-9.16}$ M at 1168 K. Note that $[H^{\bullet}]$ does not change along the axis of the reactor. However, it cannot be excluded that the hydrogen atom concentration, kinetically determined due to reactions 4 and 5, is higher. The rate constant for (8) is not known experimentally but was taken equal to twice the rate constant advanced for desubstitution of phenol by hydrogen atoms to benzene and the hydroxyl radical.

Hence, $k_8/M^{-1}\ s^{-1}$ is $10^{9.94} \exp(-6.1/RT)$.[15] Comparison of $k_8[H^{\bullet}]$ (using the equilibrium concentration) and the computed $k_{ov,DPE}$ revealed that the contribution of the induced decomposition decreased from 2% at 1123 K to 1.5% at 1168 K. Incorporating these minor corrections, we obtained $k_1/s^{-1} = 10^{15.5} \exp(-75.3/RT)$ ($r^2 = 0.992$) (see Figure 2).

An overwhelming amount of data is available describing the reactivity of (substituted) phenoxyl radicals in the liquid phase at (near) room temperature, mostly related to the antioxidant action of phenols.[16] Phenol/phenoxyl are important intermediates in high-temperature combustion chemistry of aromatics, but quantitative information regarding the dynamics in the gas phase is scarce.

Interesting kinetic information regarding phenoxyl radicals in the gas phase could be retrieved from this experiment. The phenoxyl radicals are mainly transformed through reaction 5 and 6. The rate constant for hydrogen abstraction 5 was computed by eq 9:

$$k_5 = k_6([C_6H_5OH]/[CO][H_2]) \quad (9)$$

With $k_6/s^{-1} = 10^{11.4} \exp(-44/RT)$,[17] the result is $k_5/M^{-1}\ s^{-1} = 10^{9.0} \exp(-23/RT)$ ($r^2 = 0.997$). According to this rate expression k_5 is $10^{4.62}\ M^{-1}\ s^{-1}$ at 1150 K. With $\Delta_{r,5}H_{1150}$ of 18.2 kcal mol^{-1} and $\Delta_{r,5}S_{1150}$ of -0.9 cal mol^{-1} K^{-1},[18] the rate constant for the reverse process (abstraction of the phenolic hydrogen by a hydrogen atom) becomes $k_{-5} = 10^{8.30}\ M^{-1}\ s^{-1}$,

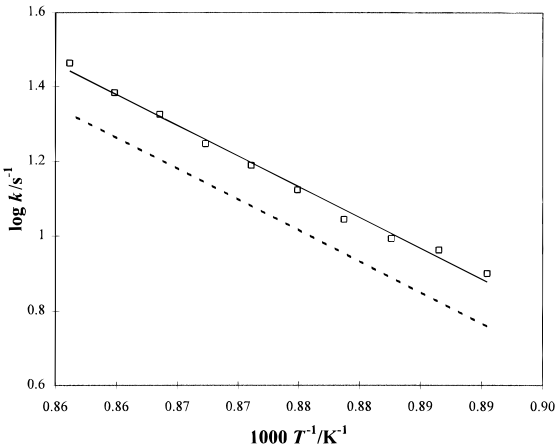

Figure 2. Unimolecular decomposition of diphenyl ether in hydrogen at atmospheric pressure: $k_1/s^{-1} = 10^{15.5} \exp(-75.3/RT)$. Dashed line: VLPP derived rate constant $k_1/s^{-1} = 10^{15.50} \exp(-75.7/RT)$.

in close agreement with a reported value of $10^{8.70}\ M^{-1}\ s^{-1}$ at that temperature.[15]

A minor process is the recombination of two phenoxyls to give dibenzofuran (DF) and *o*-hydroxybiphenyl (OHB). The ratio of these products remained constant (ca. 3:1).

$$C_6H_5O^{\bullet} + C_6H_5O^{\bullet} \rightarrow [C_{12}H_{10}O_2] \rightarrow DF/OHB \quad (10)$$

Based on DF formation only, a rate constant k_{10} could be derived using eq 11:

$$k_{10} = (k_6/[CO])^2 \tau [DF] \quad (11)$$

With the CO formation as a reference reaction for the phenoxyl concentration, k_{10} was found to be $10^{8.2}\ M^{-1}\ s^{-1}$, virtually independent of temperature. Our studies on phenoxyl recombination in the gas phase between 500 and 850 K revealed, also based on DF formation alone, a quite similar result.[5] In general, radical−radical combination rate constants[1] are mostly in the order of $10^9\ M^{-1}\ s^{-1}$ or higher. Indeed, studies in the liquid phase have shown that the rate constant for disappearance of phenoxyl through recombination is as high as $10^{9.54}\ M^{-1}\ s^{-1}$.[1] However, it should be noted that k_{10} is an overall rate constant derived on the basis of product (DF) formation, and in retrospect either the combination of two phenoxyls is a slow (reversible) process (but temperature independent) or a large fraction of the products has escaped detection. In summary, for DPE decomposition a set of consistent gas phase rate constants could be derived (see Table 1).

Thermolysis of PVE in nitrogen/hydrogen mixtures yielded an array of products such as fulvene, benzene, phenol, benzaldehyde, carbon monoxide, methane, and ethene. Small amounts of dihydrobenzofuran, acetaldehyde, ethyne, and probably cyclopentadiene were also detected. When chloromethane was present, additional chloro- and methyl-substituted products could be observed. Using $k_{ov,PVE} = -(1/\tau)\ \ln\{[PVE]_{out}/[PVE]_{in}\}$, the overall disappearance rate constant in a mixture of nitrogen/hydrogen of 20 was calculated to be $10^{12.2} \exp(-52/RT)$ (between 1061 and 1161 K; $r^2 = 0.999$). In contrast with the DPE experiments, these parameters clearly indicate a large contribution of an induced decomposition pathway.

In nitrogen/chloromethane (4.3/1) as a bath gas, the overall conversion of PVE increased from 4 to 64% between 1036 and 1161 K ($\tau \cong 10$ ms), leading to $k_{ov,PVE} = 10^{14.3} \exp(-65/RT)$ ($r^2 = 0.997$). Benzaldehyde appeared to be a key product indicative of hydrogen atom chemistry (Scheme 1). When benzaldehyde would be the sole product of the induced pathway,

TABLE 1: Experimental Kinetic Parameters

reaction	log A (s^{-1})	E_a (kcal mol^{-1})	remarks/source
1. $C_6H_5O-C_6H_5 \rightarrow C_6H_5O^\bullet + C_6H_5^\bullet$	15.5	75.3	this work/H_2
1. $C_6H_5O-C_6H_5 \rightarrow C_6H_5O^\bullet + C_6H_5^\bullet$	15.50	75.7	this work/VLPP
8. $C_6H_5OC_6H_5 + {}^\bullet H \rightarrow C_6H_6 + C_6H_5O^\bullet$	9.94	6.1	ref 15
5. $C_6H_5O^\bullet + H_2 \rightarrow C_6H_5OH + {}^\bullet H$	9.0	23	this work/H_2
6. $C_6H_5O^\bullet \rightarrow C_5H_5^\bullet + CO$	11.4	44	ref 17
10. $C_6H_5O^\bullet + C_6H_5O^\bullet \rightarrow$ DF/OHB	8.2[a]		this work/H_2
$C_6H_5OC_2H_3 \rightarrow$ products	15.50	73.3	this work/VLPP
2. $C_6H_5-OC_2H_3 \rightarrow C_6H_5^\bullet + {}^\bullet OCHCH_2$	15.20[b]	72.7[b]	see text
3. $C_6H_5O-C_2H_3 \rightarrow C_6H_5O^\bullet + {}^\bullet CHCH_2$	15.20[b]	74.0[b]	see text

[a] Based on DF formation only; see text. [b] If ratio $\nu_2/\nu_3 = 1.8$ is due to a difference in the preexponential, then log $A_2 = 15.30$, log $A_3 = 15.05$, and $E_{a,2} = E_{a,3} = 73.3$ kcal mol^{-1}.

SCHEME 1

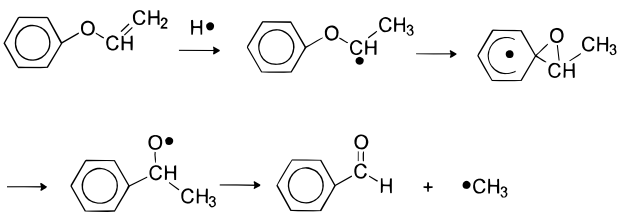

the contribution decreased from 50 to 8%. The degree of induced decomposition appeared to be almost independent of the initial [PVE] and residence time but increased with higher hydrogen/chloromethane ratios. Since the unimolecular cleavage rate was close to that of DPE (see below), induced decomposition prevailed under these experimental conditions, so no informative rate parameters for homolytic cleavage could be retrieved.

Two reasons can be mentioned for this difference in behavior relative to DPE. First, comparison of the rate constants for hydrogen atom addition to DPE (see above) or to an alkene (ethene or propene), as a model for PVE, demonstrates that the latter is at least 30 times higher.[15] Second, in the case of PVE the deviation from the equilibrium hydrogen atom concentration may be higher due to the presence of vinoxyl and vinyl. Hydrogen abstraction from H_2 or recombination with $H^\bullet$ (chain termination) will occur next to decomposition to yield additional hydrogen atoms.

Very Low-Pressure Pyrolysis of DPE and PVE: Rates. From the decrease of the abundance of the molecular ion (I) relative to I_0 at 873 K, the rate constants k_{uni} were calculated[7a] at each temperature according to $k_{uni} = k_e(I_0 - I)/I$. The escape rate constant k_e ($= 1.47(T/M)^{1/2}$, M being the molar mass of the reactant) is directly related to the geometry of the reactor (with a collision number of 9200). Under VLPP conditions the measured rate constants are in the falloff or pressure-dependent region. Hence, the RRKM algorithm[19] needs to be employed in order to obtain the kinetic expressions holding for high (infinite)-pressure conditions. The input requires, among others, the vibrational frequencies and moments of inertia for the ground state and the activated complex (see Table S1 of Supporting Information). This Stein−Rabinowith RRKM algorithm[7b] involves a purely vibrational model approach, without taking into account the presence of internal rotors. There may be a difference when these internal rotors are incorporated into the calculations. However, using alkylbenzenes[7b] and substituted anisoles[20] VLPP data, it has been shown that both approaches generated the same high-pressure values. The data for the ground state molecules were obtained from DFT calculations[21] using the Gaussian 94 package (see below). The RRKM calculation cannot yield the preexponential factor and the activation energy simultaneously. Hence, some low frequencies of the ground state vibrational model were adjusted in such a way that log A became 15.50 at 1130 K, identical to the experimental value found in our DPE/H_2 study (see above). The k_{uni} data were fitted by variation of the threshold energy to result in $k_1/s^{-1} = 10^{15.50} \exp(-75.7/RT)$ (Figure 3), in excellent agreement with the established rate expression in a hydrogen atmosphere (see Figure 2), substantiating the validity of the vibrational model as calculated by DFT and RRKM. In the case of the RRKM calculations for PVE, no attempts were made to distinguish the pathways 2 and 3, since the frequencies for the C−O stretch vibrations ($\nu_{as} = 1261.7$ cm^{-1}, $\nu_s = 1175.0$ cm^{-1}) cannot be disentangled into separate vibrations for O−phenyl and O−vinyl. With log $A = 15.50$, the overall rate expression at the high-pressure limit obeyed $k_{2+3}/s^{-1} = 10^{15.50} \exp(-73.3/RT)$ (Figure 4). The error margins in RRKM calculated activation energies were approximately 0.5 kcal mol^{-1}.

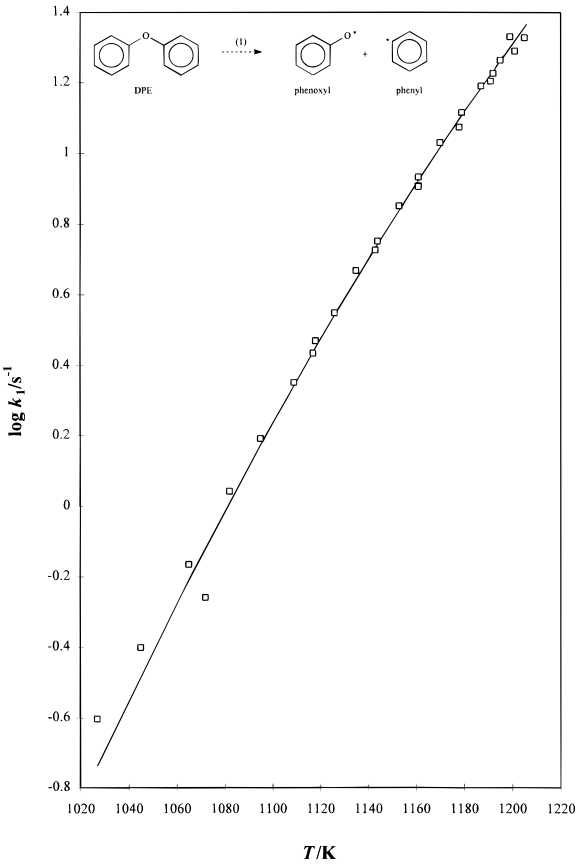

Figure 3. VLPP data for unimolecular decomposition of diphenyl ether (DPE) at 0.5 mTorr and RRKM calculations (solid line). Rate parameters: $k_1/s^{-1} = 10^{15.50} \exp(-75.7/RT)$.

Evaluation of the low-pressure data revealed that the rates of disappearance for DPE and PVE were quite similar, which was verified by an additional competition experiment. On the

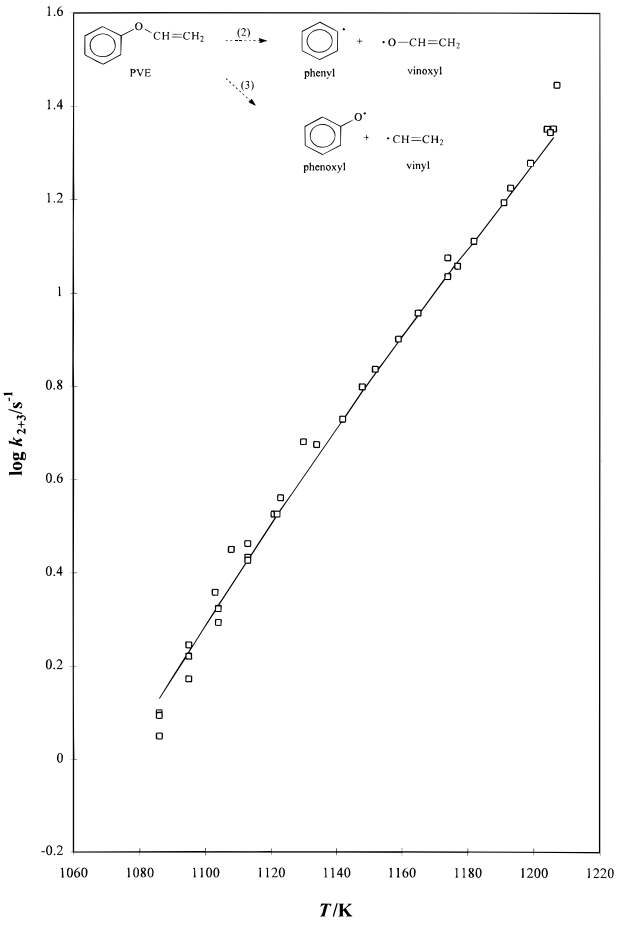

Figure 4. VLPP data for unimolecular decomposition of phenyl vinyl ether (PVE) at 0.5 mTorr and RRKM calculation (solid line). Rate parameters: $k_{2+3}/s^{-1} = 10^{15.50}\exp(-73.3/RT)$.

other hand, the homolysis rate constants at the high-pressure limit were markedly different, with $k_1 = 7.08\ s^{-1}$ and $k_{2+3} = 20.7\ s^{-1}$ at 1130 K. Moreover, reactions 1 and 2 + 3 were not identical in their falloff behavior. Over the temperature region 1100−1200 K the ratio between the low- and high (infinite)-pressure rate constant (k_{uni}/k_{inf}) ranged from 0.60 to 0.39 for DPE and from 0.25 to 0.13 for PVE. Hence, under the same conditions, PVE homolysis was already further away from the collisional stabilization. This phenomenon may originate from the relatively lower number of internal vibrational degrees of freedom.[19]

Reaction enthalpies at the thermodynamic standard state of 298 K (see Table 2) were retrieved from the activation energies according[23] to eq 12

$$\Delta_r H_{298} = E_a + 0.5RT_m - \Delta_r C_p(T_m - 298) \qquad (12)$$

in which T_m is the mean temperature of the experiment (1130 K; ca. 40% conversion) and $\Delta_r C_p$ the average change in the heat capacities of the reaction species. Since the difference (T_m−298) was quite large, an erroneous $\Delta_r C_p$ could affect the final $\Delta_r H_{298}$ considerably. For molecules and radicals containing the element oxygen, values for $\Delta_r C_p$ are not abundantly available. Therefore, they were derived from the enthalpies for reactions 1−3 at 298 and 1130 K as computed by the B3LYP/6-31(d) procedure (see below). As an alternative approach, using group increment rules,[24] ca. 50% more negative values were obtained (see Table 2, footnote *a*). Further calculations will be based on the B3LYP values.

Reaction enthalpies for (1)−(3) at 1130 and 298 K and the corresponding (experimental) heats of formation for phenoxyl, vinoxyl, phenyl, and vinyl are presented in Tables 2 and 3. With these values, BDEs in structural related compounds were derived as well (Table 4).

TABLE 2: Experimental and Computed Reaction Enthalpies in kcal mol^{-1}

	$\Delta_r H^a$ (exp)		$\Delta_r H^b$ (B3LYP)	
reaction	1130 K	298 K	1130 K	298 K
1. $C_6H_5O-C_6H_5 \rightarrow C_6H_5O^\bullet + C_6H_5^\bullet$	76.8	78.8	72.3	74.3
2. $C_6H_5-OC_2H_3 \rightarrow C_6H_5^\bullet + {}^\bullet OCHCH_2$	74.1[c]	75.9	69.9	71.7
3. $C_6H_5O-C_2H_3 \rightarrow C_6H_5O^\bullet + {}^\bullet CHCH_2$	74.8[c]	76.0	72.2	73.4
14. $C_6H_5O^\bullet + {}^\bullet CHCH_2 \rightarrow C_6H_5^\bullet + {}^\bullet OCHCH_2$	−0.7[d]	-0.1[d]	−2.3	−1.7[e]

[a] $\Delta_r H_{1130} = E_a + 0.5RT_m$ (T_m = 1130 K); $\Delta_r H_{298} = \Delta_r H_{1130} - \Delta_r C_p(T_m - 298)$, $\Delta_r C_p$ are derived from the differences in *ab initio* calculated $\Delta_r H$ values at 298 and 1130 K, to yield $\Delta_r C_p$ of −2.40 (1), −2.16 (2), and −1.44 (3) cal mol^{-1} K^{-1}. $\Delta_r C_p$ could also be estimated according to group increment rules (ref 24): −3.9 (1), −3.3 (2), and −2.5 (3). The B3LYP $\Delta_r C_p$ values were applied. [b] Computed with the B3LYP/6-31G(d) method. [c] Average based on $E_{a,2}$ = 73.3 or 72.7, $E_{a,3}$ = 73.3 or 74 kcal mol^{-1} (see Table 1 and text). [d] $\Delta_r H_2 - \Delta_r H_3$. [e] At B3LYP/6-311++G(d,p) level $\Delta_r H = -0.8$ kcal mol^{-1}.

TABLE 3: Heats of Formation ($\Delta_f H_{298}$) of Radicals, Experimental vs Literature Values, in kcal mol^{-1}

species	exp	lit. values	refs
$C_6H_5O^\bullet$	12.1[a]	11.6 ± 1.6	2
$C_2H_3O^\bullet$	2.2[b]	2.5 ± 2.2	3
$C_6H_5CH_2^\bullet$		48.4 ± 1.5	3
$C_3H_5^\bullet$		40.8 ± 2.1	3
$C_6H_5^\bullet$	79.1	78.9 ± 0.8	3
$C_2H_3^\bullet$	69.3[b]	71.6 ± 0.8	3
$H^\bullet$		52.1[c]	18

[a] From anisol thermolysis (ref 4c). [b] Average values; see Table 2. [c] Calculated by B3LYP/6-31G(d), 52.2, and by B3LYP/6-311++G(d,p), 52.3 kcal mol^{-1}.

TABLE 4: Experimental and B3LYP Computed Bond Dissociation Energies (BDE)[a] at 298 K in kcal mol^{-1}

compd	$\Delta_f H^b$	BDE[c]	BDE (B3LYP)[d]	$\Delta_r S^0$ [e]	ΔBDE[f]
C_6H_5O-H	−23.0	87.2	79.3 (83.1)	26.5	7.9 (4.1)
$C_6H_5O-C_6H_5$	12.4[g]	78.8	74.3	42.3	4.5
$C_6H_5O-C_2H_3$	5.4	76.0	73.4	40.6	2.6
C_2H_3O-H	−30.0	84.3	74.8 (79.8)	27.2	9.5 (5.4)
$C_2H_3O-C_6H_5$	5.4	75.9	71.7	42.6	4.2
$C_2H_3O-C_2H_3$	−3.0	74.5	72.5 (69.1)[h]	43.6	2.0 (5.4)
C_6H_5-H	19.8	111.4	110.9 (110.6)	33.6	0.5 (0.8)
C_2H_3-H	12.5	108.9	109.3 (108.3)	30.9	−0.4 (0.6)
$C_6H_5CH_2-H$	12.0	88.5	87.9	23.2	0.6
$C_6H_5CH_2-C_6H_5$	39.7	87.8[i]			
$C_6H_5CH_2-C_2H_3$	32.6	85.1	82.8	41.6	2.3
C_3H_5-H	4.8	88.1	85.1 (84.1)	25.8	3.0 (4.0)
$C_3H_5-C_6H_5$	32.6	87.3	80.6	41.3	6.7

[a] Defined as BDE(R−X) = $\Delta_r H_{298} = \Delta_r H(R^\bullet) + \Delta_r H(X^\bullet) - \Delta_r H(RX)$. [b] From NIST SP (ref 18) in kcal mol^{-1}. [c] Using experimental heats of formation or if not available literature data as given in Table 3. [d] B3LYP/6-31G(d), in parentheses B3LYP/6-311++G(d,p). [e] Computed by B3LYP/6-31G(d) and defined as $\Delta_r S^0 = S^0(R^\bullet) + S^0(X^\bullet) - S^0(RX)$ in cal mol^{-1} K^{-1}. [f] ΔBDE = BDE(exp) − BDE (computed). [g] Reference 25. [h] Ground state confomer: *s-trans, s-trans*. [i] A VLPP study (ref 26) with $C_6H_5CH_2C_6H_5$ ($\rightarrow C_6H_5CH_2^\bullet + C_6H_5^\bullet$) produced a BDE of 86.7 kcal mol^{-1} at 298 K.

Very Low-Pressure Pyrolysis of DPE and PVE: Products. With the VLPP instrument, the products detected were mainly the molecules instead of the radical species. Thus, the phenyl radical (*m/z* = 77) was converted largely into benzene (*m/z* = 78) before arriving at the analyzer by means of (wall-associated) hydrogen transfer reactions. Likewise, phenoxyl (*m/z* = 93) could incorporate a hydrogen from the wall to give phenol (*m/z* = 94) but predominantly decomposed (reaction 6) into CO (*m/z*

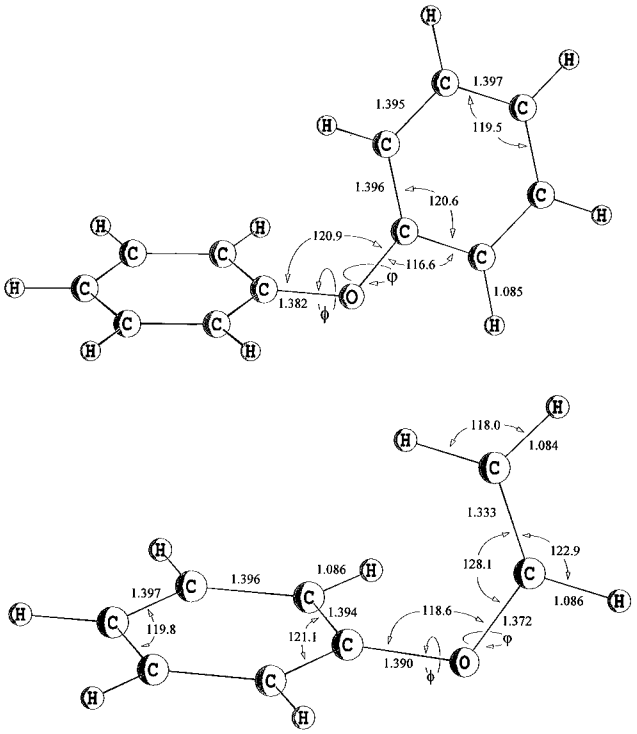

Figure 5. B3LYP/6-31G(d) optimized structures and selected geometrical parameters of diphenyl ether and phenyl vinyl ether.

= 28) and the cyclopentadienyl radical (*m/z* = 65). The last species was converted into cyclopentadiene (*m/z* = 66). A small difference between PVE and DPE was observed in the ratio *m/z* = 94/(65 + 66): 0.9−1.1 and 0.6−0.7 at 1130 K as well as for *m/z* = 66/65 (6−14 and 5−10). Assuming that the increase in *m/z* = 94 is due to additional formation of phenol (see Discussion), a decrease in the ratio *m/z* = 66/65 can be expected as this ratio is close to unity for the fragmentation of phenol in the ionization chamber. Therefore, the relative increase in *m/z* = 94 is rationalized by the presence of more reactive hydrogen-donating species, and indeed, the vinoxyl radical is known to be a hydrogen donor.[7c] In the case of DPE the molar phenyl/phenoxyl product ratio should be directly proportional to the abundance ratio, $I_{b(enzene)/p(henol)}$, of the corresponding molecular ions ($(I_{77} + I_{78})/(I_{94} + I_{93} + I_{65} + I_{66})$). Experimentally, $I_{b/p}$ increased from 0.8 to 1.2. Small differences in the ionization efficiencies of the species could be the reason for the deviation from unity. Moreover, the composition of the exit product stream fluctuated with temperature due to the enhanced thermal degradation of the phenoxyl radicals. Since DPE and PVE decomposed in the same temperature region, the $I_{b/p}$ from the DPE experiments were used as calibration factors to determine the molar phenyl/phenoxyl ratio (the branching ratio for reaction 2 and 3, v_2/v_3) during the homolysis of PVE. Accordingly, between 1050 and 1100 K the ratio v_2/v_3 changed from 2.3 to 1.8, and remained constant from 1100 to 1200 K (25−80% conversion of PVE).

Another expected product from the PVE decomposition, C_2H_4 (from $C_2H_3^\bullet$), was obscured by CO (*m/z* = 28), and vinoxyl formation was qualitatively observed as ketene (CH_2CO) and acetaldehyde. It was noticed that at pressures above 1.5 mTorr benzaldehyde was showing up as a product, indicating other (bi)molecular reactions.

Density Functional Theory Calculations. The computed minimum structures and selected geometrical parameters of DPE and PVE are displayed in Figure 5. Selecting the reference plane through one of the phenyl groups of DPE, the twisting angle ϕ around the corresponding phenyl−O bond amounts to ca. 40°, with the plane of the other phenyl group forming an angle φ of about 68° with the reference plane. These data are in good agreement with the experimental gas phase structure (angles of 29° and 70°, respectively).[27] The computed central C−O−C angle (120.9) is slightly wider than the experimental one (116 ± 5°). The oxygen is predicted to be slightly (3.3°) bent out of the phenyl reference plane.

In PVE the vinyl group is significantly more twisted out of the phenyl plane (dihedral angle $\phi = 85.6°$), with the plane of the vinyl group almost perpendicularly ($\varphi = 85°$) oriented with respect to the phenyl plane. Optimized geometries and vibrational frequencies for DPE and PVE were used for RRKM calculations (Table S2 of Supporting Information).

Absolute electronic energies, zero-point vibrational energies (ZPVE), were the basis of the calculations of $\Delta_r H$ for (1)−(3) at 298 and 1130 K (see Table 2). In order to obtain more insight into the quality of the computations, the BDEs of interest (including the corresponding reaction entropies $\Delta_r S^0$) in ethene (vinyl), benzene (phenyl), propene (allyl), toluene (benzyl), vinyl alcohol (vinoxyl), phenol (phenoxyl), divinyl ether, and allylbenzene (as hydrocarbon analogous for PVE) were calculated as well (see Table 4).

Discussion

Rates. The overall kinetic parameters for PVE involve the cleavage into phenyl and vinoxyl (2) and into phenoxyl and vinyl (3). Next to these two homolytic pathways, an additional reaction channel may be operative: the concerted 1,2 elimination toward phenol and ethyne (13).

$$C_6H_5OC_2H_3 \rightarrow C_6H_5OH + C_2H_2 \qquad (13)$$

Whether or not the direct elimination plays an important role under our reaction conditions can be decided on the basis of thermokinetic grounds and experimental evidence. For the saturated analogue of PVE, ethyl phenyl ether, three independent studies[20,28] have shown that within experimental error the concerted elimination to phenol and ethene does not take place. With *n*-butyl phenyl ether, the direct molecular elimination toward phenol and 1-butene has been parametrized as $\log k/s^{-1} = 10^{13.60} \exp(-57.4/RT)$. The observed activation energy (E_a) can be related to the intrinsic activation energy ($E_{a,int}$), associated with the concerted elimination, and the reaction enthalpy ($\Delta_r H$): $E_a = E_{a,int} + \Delta_r H$. With $\Delta_r H$ of 13 kcal mol^{-1}, the $E_{a,int}$ becomes 44 kcal mol^{-1}, a value which is quite common for 1,2 elimination processes involving oxygen (e.g., $C_2H_5OR \rightarrow C_2H_4 + ROH$).[15,18] When this value is applied to PVE ($\Delta_r H$ = 26 kcal mol^{-1}), the rate parameters for the 1,2 elimination in PVE become $\log k_{13}/s^{-1} = 10^{13.60} \exp(-70/RT)$. According to this analysis, the contribution of the concerted pathway 13 to the overall rate of disappearance for PVE could range between 1100 and 1200 K from 5.5 to 5%. Through the presence of a molecular pathway the relative amount of phenol should be increased. However, the small change in the VLPP product pattern between PVE and DPE (see Results) can already be rationalized by the increased amount of hydrogen-donating species (e.g., disproportionation) in the gas mixture: vinoxyl and vinyl. Therefore, it can be concluded that under the experimental conditions reaction 13 plays at best a minor role.

Above 1100 K the observed branching ratio, v_2/v_3, is found to be 1.8 with no apparent temperature variation and can be related to an enthalpic or an entropic effect on activation. Supposing that the preexponential factors are identical (see Table 1), this ratio would correspond to an energy difference of 1.3 kcal mol^{-1} at 1130 K and hence $E_{a,2}$ = 72.7 kcal mol^{-1} and

$E_{a,3}$ = 74.0 kcal mol^{-1}. Consequently, the change in υ_2/υ_3 between 1100 and 1200 K would be from 1.81 to 1.78 which, given the experimental uncertainties, may well have escaped detection. On the other hand, when the E_as are identical, the overall preexponential can be separated into two A values on the basis of $\upsilon_2/\upsilon_3 = 1.8$. This leads to log A_2 = 15.30 and log A_3 = 15.05, corresponding to $\Delta S_2^{\ddagger} - \Delta S_3^{\ddagger}$, the differences between the ground state and the two transition states, of 1.17 eu at 1130 K.

No further conclusive (entropic or enthalpic) evidence is available to support either scenario. Hence, since the variation in the respective E_as is relatively small ($E_{a,2}$ = 72.7 or 73.3 kcal mol^{-1}, $E_{a,3}$ = 74.0 or 73.3 kcal mol^{-1}) and is close to the overall experimental error (ca. 0.5 kcal mol^{-1}), further thermodynamic evaluation will be based on the average values for the routes, i.e., $E_{a,2}$ = 73.0 and $E_{a,3}$ = 73.7 kcal mol^{-1}. For a homolytic cleavage process the enthalpy of activation is directly related to the strength of the bond, provided that the reverse reaction (combination of two radicals) has no activation barrier. Hence, by extrapolation of these kinetic data to T = 298 K (see Table 2), it is found that in PVE the phenyl−vinoxyl and the phenoxyl−vinyl bonds are quite comparable, i.e., 75.9 and 76.0 kcal mol^{-1}, respectively (see Table 4).

The high-pressure (overall) rate constants for PVE and DPE show a clear difference in their temperature dependence (see Table 1). Combination with the experimental branching in PVE of 1.8, the ratio of rate constants (per bond) at 1130 K becomes k_3:k_1 = 2.08. The difference in E_a between (3) and (1) becomes 1.7 kcal mol^{-1} (log A_3 = 15.20) or 2.4 kcal mol^{-1} (log A_3 = 15.05). Thus, using the average value, the phenoxyl−phenyl bond is 2.0 kcal mol^{-1} stronger than the phenoxyl−vinyl bond at 1130 K. Extrapolation to 298 K slightly increases this difference to 2.8 kcal mol^{-1} (see Tables 2 and 4).

Thermodynamic Quantities. On the basis of the average experimental activation energies, heats of formation of the radicals vinoxyl and phenyl are in accordance with the recommended values, while the $\Delta_f H$ for vinyl is clearly lower (see Table 3). As a consequence and in contrast with the previous assumption, as stated in the Introduction, the C−H bonds in ethene and benzene are not equally strong. A part of the discrepancy can be found in the way the literature data has been compiled in ref 3, which learns that the BDE(C−H) in ethene ranges from 105 to 110 kcal mol^{-1}, depending on the experimental technique used. Our value for the C−H bond strength in benzene is almost identical with the recommended literature value, which also gives assurance as to the applied method of B3LYP ΔC_p corrections. In this study it has been found that loss of vinyl from PVE is faster than loss of phenyl in DPE, and as a consequence, these carbon−oxygen bonds cannot be equally strong. The obtained $\Delta_f H$, after B3LYP ΔC_p corrections, for the vinoxyl radical (the other reaction channel for PVE) again tallies very well with other studies. Hence, from this work the conclusion can be drawn that $\Delta_f H_{298}(C_2H_3^{\bullet})$ = 69.3 kcal mol^{-1}, and consequently the C−H bond in ethene is 2.5 kcal mol^{-1} weaker than in benzene.

Both phenoxyl and vinoxyl belong to the group of resonance-stabilized radicals. The radical stabilization energies (RSE) in a compound of the type ROH can be defined as RSE = BDE(O−H)$_{ref}$ − BDE(O−H)$_{ROH}$. When taking as a reference the BDE(O−H)$_{ref}$ of 105 kcal mol^{-1} in a saturated alcohol,[18] the RSE reaches 18 and 21 kcal mol^{-1} for phenol and vinyl alcohol, respectively. Electron spin resonance (ESR) data and the unpaired spin density distribution obtained from our calculations show that the delocalization of the free electron in vinoxyl is slightly more pronounced, and hence the magnitude of the RSE is proportional to the degree of "non-oxygen character" of the two radicals. On the other hand, for the hydrocarbons such as toluene and propene (see Table 4), the allylic and benzylic RSE are almost identical (13 kcal mol^{-1}, using the BDE(C−H) in C_2H_6 of 101 kcal mol^{-1}).[3] This equivalence has also been observed for the cyclic analogous compounds tetralin and cyclohexene.[29] ESR measured and calculated spin densities[30] show that the degree of delocalization is slightly (by a factor of about 1.13) better in allyl than in benzyl. Provided that this is the determining feature, the expected difference in the BDE(C−H) for propene and toluene may well be within the experimental uncertainties.

Experimental vs Calculated Reaction Enthalpies. This study provides the opportunity to compare and evaluate the discrepancies between experimental and DFT calculated data. It should be noticed that experimental thermodynamic values always include assumptions, uncertainties, and in most cases extrapolations to T = 298 K. Moreover, some literature data for $\Delta_f H$ of organic compounds originate from group additivity rules rather then from actual experimental determination. The B3LYP computed BDE (C−H) in the hydrocarbons (Table 4) ethene, benzene, propene, and toluene are in (almost) perfect agreement with the experimental data, except for propene. However, deviations outside any experimental uncertainty become visible when the element oxygen is incorporated in the reaction. In this case computations at a higher level gives better results, although still an underestimation of the BDE(O−H) and BDE(O−C) is found. A similar effect has been reported for the BLYP DFT procedure.[31] For example, the computed BDE(O−H) in vinyl alcohol differs 5.4 kcal mol^{-1} from the experiment. By way of contrast, the deviation between experimental and B3LYP/6-31G(d,p)-calculated C−H BDE in acetaldehyde (to give the identical vinoxyl radical) is significantly smaller, 0.8 kcal mol^{-1}.[22]

The same effect is observed in the DFT calculations of the C−H and O−H bond strength in CH_3OH: while BDE(C−H) matches well, the BDE(O−H) is 99 instead of the expected 105 kcal mol^{-1}.[18] Hence, the bonding of oxygen with other elements appears to be not well parametrized. For the metathesis process (reaction 14), which involves only radicals, the $\Delta_r H_{298}$ difference between the experiment and the B3LYP calculation amounts to 1.6 kcal mol^{-1} with 6-31G(d) or 0.7 kcal mol^{-1} with 6-311++G(d,p), again in close agreement.

$$C_6H_5O^{\bullet} + {}^{\bullet}C_2H_3 \rightarrow C_6H_5^{\bullet} + {}^{\bullet}OC_2H_3 \qquad (14)$$

Hence, it can be concluded that a large portion of the discrepancy in the DFT procedure originates from the calculation of the $\Delta_f H$ for the oxygen-containing molecules. Whether or not this is a systematic error remains uncertain. DFT computational methods have been applied to validate the substituent effect on the strength of the O−CH_3 bonds in a series of anisole derivatives.[31] Computed enthalpy differences between the R−$C_6H_4OCH_3$ and the substituted phenoxyl radicals, R-$C_6H_4O^{\bullet}$, disclosed the proportions of ground state and product radical stabilization effects as a function of R. However, a verification of the computed $\Delta_f H$ of the reactants remains necessary to ensure that the relative increment due to the change in R is properly incorporated by the computation.

Computations on the two C−C bonds (reactions 15 and 16) in allylbenzene (the hydrocarbon analogous of PVE) are not in accordance with expected reaction enthalpies, mainly because the apparent stabilization energy in the calculated allyl radical is too high.

$$C_6H_5\text{-}C_3H_5 \rightarrow C_6H_5^{\bullet} + {}^{\bullet}C_3H_5 \quad (15)$$

$$C_6H_5CH_2\text{-}C_2H_3 \rightarrow C_6H_5CH_2^{\bullet} + {}^{\bullet}C_2H_3 \quad (16)$$

In general, the DFT calculated entropy changes (and hence heat capacities) for the dissociation reactions (see Table 4) are more consistent with other experimental sources. Hence, the vibrational molecular models of these compounds are well-characterized.

Conclusions

The experimental data show that the two carbon−oxygen bond strengths in PVE are only slightly different at 298 K. This originates from a compensation effect since, in terms of X−H, the C−H bond in ethene is 2.5 kcal mol^{-1} stronger relative to benzene, while the O−H bond in vinyl alcohol is 2.9 kcal mol^{-1} weaker than in phenol. The phenoxyl−vinyl bond (in PVE) is 2.8 kcal mol^{-1} weaker than the phenoxyl−phenyl bond (in DPE) at 298 K.

The experimental and computed C−O and O−H bond strengths appear to be not identical. Density functional theory at B3LYP/6-31G(d) or higher level underestimates these dissociation energies by ca. 5 kcal mol^{-1}. A further optimization of the DFT method is required to ensure proper treatment of bonds involving the element oxygen. Computation of the BDE(C−H) reveals a quite smaller deviation from experimental data.

This study shows the synergism between experimental and computational methods. Thermal techniques, such as VLPP, require accurate vibrational frequencies to correct for the falloff behavior and reliable heat capacity data to extrapolate to 298 K; both can be obtained by DFT calculations.

Acknowledgment. We thank the Hochschulrechenzentrum der Universität Essen for generous allotment of computation time and Willi Sicking, Guido Hulstman, and Louw van As for technical assistance.

Supporting Information Available: Tables of applied RRKM parameters and optimized geometries and vibrational frequencies for DPE and PVE (2 pages). Ordering information is given on any current masthead page.

References and Notes

(1) Arends, I. W. C. E.; Mulder, P.; Clark, K. B.; Wayner, D. D. M. *J. Phys. Chem.* **1995**, *99*, 8182−8189.

(2) Wayner, D. D. M.; Lusztyk, E.; Pagé, D.; Ingold, K. U.; Mulder, P.; Laarhoven, L. J. J.; Aldrich, H. S. *J. Am. Chem. Soc.* **1995**, *117*, 8737−8744.

(3) Berkowitz, J.; Ellison, G. B.; Gutman, D. *J. Phys. Chem.* **1994**, *98*, 2744−2765.

(4) (a) Schraa, G.-J.; Arends, I. W. C. E.; Mulder, P. *J. Chem. Soc., Perkin Trans. 2* **1994**, 189−197. (b) Meurs, M.; Arends I. W. C. E.; Louw, R.; Mulder, P. *Recl. Trav. Chim. Pays-Bas* **1991**, *110*, 475−479. (c) Arends, I. W. C. E.; Louw, R.; Mulder, P. *J. Phys. Chem.* **1993**, *97*, 7914−7925. (d) Dorrestijn, E.; Pugin, R.; Ciriano Nogales, M. V.; Mulder, P. *J. Org. Chem.*, in press.

(5) Born, J. G. P. Thesis, Leiden University, 1992.

(6) Poutsma, M. L. A Review of Thermolysis Studies of Model Compounds Relevant to Processing of Coal, Report ORNL/TM-10637, 1987.

(7) (a) Golden, D. M.; Spokes, G. N.; Benson, S. W. *Angew. Chem., Int. Ed. Engl.* **1973**, *12*, 534−546. (b) Robaugh, D. A.; Stein, S. E. *Int. J. Chem. Kinet.* **1981**, *13*, 445−462. (c) Rossi, M.; Golden D. M. *Int. J. Chem. Kinet.* **1979**, *11*, 715−729.

(8) McClelland, R. A. *Can. J. Chem.* **1977**, *55*, 548−551.

(9) (a) Labanowski, J. K.; Andzelm, J. W., Eds. *Density Functional Methods in Chemistry*; Springer: New York, 1991. (b) Parr, R. G.; Yang, W. *Density Functional Theory of Atoms and Molecules*; Oxford University Press: Oxford, 1989. (c) Ziegler, T. *Chem. Rev.* **1991**, *91*, 651−667. (d) Jones, R. O.; Gunnarsson, O. *Rev. Mod. Phys.* **1989**, *61*, 689−746. (e) Seminario, J. M.; Politzer, P. *Modern Density Functional Theory: A Tool for Chemistry*; Elsevier: Amsterdam, 1995.

(10) Frisch, M. J.; Trucks, G. W.; Schlegel, H. B.; Gill, P. M. W.; Johnson, B. G.; Robb, M. A.; Cheeseman, J. R.; Keith, T.; Petersson, G. A.; Montgomery, J. A.; Raghavachari, K.; Al-Laham, M. A.; Zakrzewski, V. G.; Ortiz, J. V.; Foresman, J. B.; Cioslowski, J.; Stefanov, B. B.; Nanayakkara, A.; Challacombe, M.; Peng, C. Y.; Ayala, P. Y.; Chen, W.; Wong, M. W.; Andres, J. L.; Replogle, E. S.; Gomperts, R.; Martin, R. L.; Fox, D. J.; Binkley, J. S.; Defrees, D. J.; Baker, J.; Stewart, J. P.; Head-Gordon, M.; Gonzalez, C.; Pople, J. A. *Gaussian 94, Revision C.3*; Gaussian, Inc.: Pittsburgh, PA, 1995.

(11) (a) Becke, A. D. *Phys. Rev. A* **1988**, *38*, 3098−3100. (b) Becke, A. D. *J. Chem. Phys.* **1993**, *98*, 5648−5652. (c) Lee, C.; Yang, W.; Parr, R. G. *Phys. Rev. B* **1988**, *37*, 785−789.

(12) Scott, A. P.; Radom, L. *J. Phys. Chem.* **1996**, *100*, 16502−16513.

(13) Arends, I. W. C. E. Thesis, Leiden University, 1993.

(14) Manion, J. A.; Louw, R. *J. Phys. Chem.* **1989**, *93*, 3563−3574.

(15) Mallard, W. G.; Westley, F.; Herron, J. T.; Hampson, R. F. *NIST Chemical Kinetics Database*, version 5.0; NIST Standard Reference Data; National Institute of Standards and Technology: Gaithersburg, MD, 1993.

(16) (a) Mahoney, L. R.; DaRooge, M. A. *J. Am. Chem. Soc.* **1975**, *97*, 4722−4731. (b) Foti, M.; Ingold, K. U.; Lusztyk, J. *J. Am. Chem. Soc.* **1994**, *116*, 9440−9447. (c) Lucarini, M.; Pedrielli, P.; Pedulli, G. F.; Cabiddu, S.; Fattuoni, C. *J. Org. Chem.* **1996**, *61*, 9259−9263.

(17) Lin, C.-Y.; Lin, M. C. *J. Phys. Chem.* **1986**, *90*, 425−431.

(18) Stein, S. E.; Rukkers, J. M.; Brown, R. L. *NIST Structures and Properties Database*, version 2.0; NIST Standard Reference Data; National Institute of Standards and Technology: Gaithersburg, MD, 1994.

(19) Gilbert, R. G.; Smith, S. C. *Theory of Unimolecular and Recombination Reactions*; Blackwell Scientific Publications: Oxford, 1990.

(20) Suryan, M. M.; Kafafi, S. A.; Stein, S. E. *J. Am. Chem. Soc.* **1989**, *111*, 1423−1429.

(21) For the RRKM calculation B3LYP frequencies were adjusted by a factor of 0.97 (see refs 12 and 22). The Gaussian output revealed that low frequencies might be due to hindered internal rotation. PVE: 19.02, 161.5, 425.05 cm^{-1}; DPE: 22.6, 90.2, 422.6, 426.6, 489.2 cm^{-1}. This may produce slight errors in heat capacity calculations (see ref 10).

(22) Korth, H.-G.; Sicking, W. *J. Chem. Soc., Perkin Trans 2* **1997**, 715−719.

(23) Smith, G. P.; Manion, J. A.; Rossi, M. J.; Rodgers, A. S.; Golden, D. M. *Int. J. Chem. Kinet.* **1994**, *26*, 211−217.

(24) Ritter, E. R.; Bozelli, J. W. *Int. J. Chem. Kinet.* **1991**, *23*, 767−778.

(25) Pedley, J. B.; Naylor, R. D.; Kirby, S. P. *Thermochemical Data of Organic Compounds*, 2nd ed.; Chapman and Hall: New York, 1986.

(26) Rossi, M. J.; McMillen, D. F.; Golden, D. M. *J. Phys. Chem.* **1984**, *88*, 5031−5039.

(27) Naumov, V. A.; Ziatchinova, R. N. *Russ. J. Struct. Chem.* **1984**, *25*, 77−81.

(28) (a) Colussi, A. J.; Zabel, F.; Benson, S. W. *Int. J. Chem. Kinet.* **1977**, *9*, 161−178. (b) Walker, J. A.; Tsang, W. *J. Phys. Chem.* **1990**, *94*, 3324−3327.

(29) Laarhoven, L. J. J.; Mulder, P. *J. Phys. Chem. B* **1997**, *101*, 73−77.

(30) Fisher, H.; Hellwege, K. H., Eds. *Landolt-Börnstein, New Series; Magnetic Properties of Free Radicals*; Springer: Berlin, 1977; Vol. II/9b, pp 342, 543.

(31) Wu, Y.-D.; Lai, D. K. W. *J. Org. Chem.* **1996**, *61*, 7904−7910.